# Why H Atom Prefers the On-Top Site and Alkali Metals Favor the Middle Hollow Site on the Basal Plane of Graphite

**Zhong Hua Zhu,* Gao Qing Lu, and Fu Yang Wang**

*ARC Centre for Functional Nanomaterials, School of Engineering, University of Queensland, QLD 4072, Australia*

*Received: December 9, 2004; In Final Form: February 8, 2005*

In this work, the different adsorption properties of H and alkali metal atoms on the basal plane of graphite are studied and compared using a density functional method on the same model chemistry level. The results show that H prefers the "on-top site" while alkali metals favor the "middle hollow site" of graphite basal plane due to the unique electronic structures of H, alkali metals, and graphite. H has a higher electronegativity than carbon, preferring to form a covalent bond with C atoms, whereas alkaline metals have lower electronegativity, tending to adsorb on the highest electrostatic potential sites. During adsorption, there are more charges transferred from alkali metal to graphite than from H to graphite.

## Introduction

Hydrogen adsorption on carbon materials is important in many areas such as semiconductor technology, astrophysics, plasma surface interactions in controlled fusion devices called tokamaks, and hydrogen storage. Hydrogen adsorption on the basal plane of graphite has been extensively studied in the past several decades using various semiempirical and ab initio methods.[1−7] It is generally agreed that the H atom is preferentially adsorbed on the "on-top site" directly above a carbon atom (referred to as the *t* site), while the adsorption on the "bridging site" above a carbon−carbon bond (referred to as the *b* site) is metastable and H atom adsorption on the "middle hollow site" above a hexagonal aromatic ring may be the least favorable. More details can be found in our recent review.[8]

On the other hand, the adsorption of alkali metals on carbons plays an important role in catalyzed carbon gasifications, and lithium adsorption on nanostructured carbon materials is also a key step in lithium battery. It was also reported that alkali metals could significantly increase hydrogen storage in carbon materials,[9] but later on such an increase was found to be caused by moisture instead of hydrogen.[10,11] Unlike H atom adsorption, alkali metal atoms such as Li, Na, and K all prefer the "middle hollow site" above a hexagonal aromatic ring (referred to as the *m* site) of a single graphite layer, which has been shown by Janiak et al.,[12] Lamoen et al.,[13] and Kurita [14] as well as our recent work.[15]

Now a very important fundamental question arises, that is, why H atom prefers the "on-top site" while the "middle hollow site" is the favorite for alkali metal adsorption. In our recent study,[15] we raised such a question, but could not provide a satisfactory explanation. To the best of our knowledge, such an explanation is not available so far. No report has appeared on the comparison of H and alkali metal adsorption on graphite using the same electronic structural method either.

In this work, we address this question by studying the adsorption properties of H and alkali metal atoms on the basal plane of graphite using a density functional method with the same model chemistry level. This will lead to a plausible explanation of why H prefers the "on-top site" while alkali metals favor the "middle hollow site" site based upon the electronic structures of the H, alkali metals, and graphite. As Li, Na, and K all prefer the *m* site,[15] we just choose Li as a representative to study the adsorption of alkali metals in this work.

## Calculations

Gaussian 98[16] was used to undertake the molecular orbital theory calculations. The detailed methodology for the calculations is described elsewhere.[17] As the spin contamination could be significant from the Hartree−Fock theory method in the investigation of a single graphite sheet, and density function theory can effectively overcome the spin contamination in graphite reaction and provide more accurate results,[18] the latter was used in this study. B3LYP/3-21g(d,p) was used for geometry optimization and frequency calculation, and B3LYP/6-31g(d,p) was used for SCF (self-consistent field) energy calculations. The p functions are specifically added to hydrogen atoms in the basis set; thus 3-21g(d,p) and 6-31g(d,p) are used in the present calculations. Such a configuration can produce a good balance between calculation accuracy and computational time.[19] The spin multiplicity of each compound for the open-shell structures was determined by the same method by Kyotani and Tomita.[20] Briefly, the selected multiplicity should lead to a chemically reasonable molecular structure with the smallest spin contamination. When these conditions are satisfied, the multiplicity giving the most energetically stable state is selected.

The heat of adsorption ($\Delta H$) was determined as the difference between the total energy of the optimized system and the sum of the energies of the corresponding graphite model and gas molecules. The energy of adsorption ($E_{abs}$) is negative $\Delta H$.

Janiak et al.[12] and Lamoen et al.[13] both reported that the difference of K adsorption on single layer graphite and multilayers graphite is negligible. Barone et al.[4] and Ferro et al.[7] also found that hydrogen atom adsorption on the basal plane of graphite is a local phenomenon. Therefore, we choose single layer graphite for the purpose of mechanism study.

## Results and Discussion

Three types of adsorption sites on a single layer graphite are investigated: (1) the "on-top site" directly above a carbon atom

* Corresponding author. E-mail: johnz@cheque.uq.edu.au.

10.1021/jp044407s CCC: $30.25 
Published on Web 03/30/2005

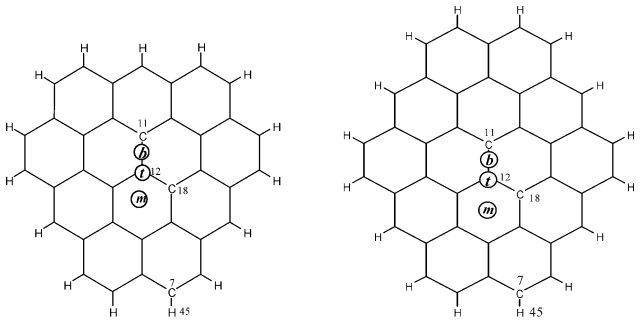


**Figure 1.** Three types of adsorption sites on a single graphite sheet.

(called *t* site); (2) the "bridging site" above a carbon−carbon bond (called *b* site); and (3) the "middle hollow site" above a hexagon (called *m* site). These different sites are illustrated in Figure 1. In this figure, model 1-A has an odd electron number with an open-shell electronic state, and model 1-B has an even electron number with a closed-shell electronic state. These two models will be calculated separately to test different spin states at minima.

The adsorption data of H atom on models 1-A and 1-B of Figure 1 are shown in Table 1. The minimal state of H atom adsorption on model 1-A following a geometry optimization is on the "on-top site" directly above a carbon atom, or the *t* site. We could not locate any optimized structure with H atom on the *m* or *b* site of model 1-A. Even though the H atom is put on the *m* or *b* site in the initial input structure, the H atom eventually moves to the *t* site after the optimization. The slightly positively charged H atom after adsorption on model 1-A indicates the charge transfer from H atom to the anchoring carbon atom C(12). The adjacent C−C bond of the anchoring C(12) of model 1-A is ca. 1.42 Å before H adsorption, which is consistent with the experimental data,[21] and is lengthened to ca. 1.51 Å after H adsorption.

Different from the adsorption on model 1-A, we did locate an optimized structure with H adsorption on both *t* and *b* sites of model 1-B, but the minimal state of H adsorption on model 1-B is still on the *t* site, and the adsorption on the *b* site is the first-order saddle point. During our IRC calculation (the results are too long and not shown in this paper), the H atom adsorbed on the *b* site goes to the two adjacent *t* sites, confirming that the *b* site adsorption is the right transition state connecting the minimal adsorption states on the two adjacent *t* sites. We could not locate any optimized structure with H atom adsorbed on the *m* site of model 1-B. Similar results were reported by Caballol et al.,[3] Barone et al.,[4] and Ferro et al.[7] The bond lengths of model 1-B are very close to that of model 1-A before and after the hydrogen adsorption on the *t* site despite that the adsorption energy of H on model 1-A is higher due to its open-shell electronic state. The adsorption energies of H on both *t* and *b* sites of model 1-B in the current study are very close to those found by Ferro et al.,[7] but very different from that by Caballol et al.[3] and Barone et al.[4] Ferro et al. also used a density functional theory method and a basis set equivalent to 6-31g(d). Caballol et al. used the MINDO (modified intermediate neglect of differential overlap) method and the calculated energy difference between *b* and *t* site adsorption was only ca. 8.4 kJ/mol, while Barone et al. used MNDO (modified neglect of diatomic overlap) and HF/STO-3G (HF means Hartree−Fock) methods and the calculated difference of adsorption energy on *b* and *t* sites was ca. 300 kJ/mol. Apparently, the semiempirical or ab initio method with very low level model chemistry, used by the latter two groups, produced large errors.

The adsorption data of the Li atom on models 1-A and 1-B such as adsorption energies, charges of metals, and bond lengths after energy optimization are presented in Table 2. On model 1-A, we also located the first- and second-order transition states with Li adsorbed on *b* and *m* sites, respectively. However, on model 1-B, only the minimal state with Li adsorbed on the *m* site is found. As with H atom adsorption, the adsorption energy of Li on model 1-B is much lower than that on model 1-A, and the bond length between metal and the graphite plane is also longer on the former than on the latter, mainly due to the latter's odd electron number with open-shell electronic state.

Li adsorption is different from H adsorption mainly in the following three aspects: (1) The *m* site is the most energetically

**TABLE 1: Adsorption Data of One Single Hydrogen Atom Adsorption on Models 1-A and 1-B in Figure 1**

| | bond data | | charge of the adsorbed H atom and the anchoring atom C(12) (based upon sum of Mulliken charges = 0) | $E_{ads}$ (kJ/mol H) | number of imaginary frequency |
|---|---|---|---|---|---|
| | bond name | bond length (Å) | | | |
| model 1-A | C(12)−C(11) | 1.425 | C(12): +0.0968 | | 0 |
| | C(12)−C(18) | 1.425 | | | |
| single H on *t* site of model 1-A | C(12)−H | 1.106 | H: +0.1623 | 154 | 0 |
| | | | C(12): +0.2807 | | |
| | C(12)−C(11) | 1.516 | | | |
| | C(12)−C(18) | 1.516 | | | |
| model 1-B | C(12)−C(11) | 1.411 | C(12): +0.07870 | | 0 |
| | C(12)−C(18) | 1.429 | | | |
| H on *t* site of model 1-B | C(12)−H | 1.110 | H: +0.1616 | 80 | 0 |
| | C(12)−C(11) | 1.511 | C(12): −0.2979 | | |
| | C(12)−C(18) | 1.515 | | | |
| H on *b* site of model 1- B | C(12)−H or C(11)−H | 1.32 | H: +0.2526 C(12): −0.1837 | −63[a] | 1 |
| | C(12)−C(11) | 1.49 | | | |
| | C(12)−C(18) | 1.44 | | | |

[a] The negative adsorption energy means the adsorption is endothermic.

**TABLE 2: Adsorption Data of One Single Li Atom on Models 1-A and 1-B in Figure 1**

| | | $E_{ads}$ (kJ/mol Li) | charges of Li (based upon sum of Mulliken charges = 0) | $d$[M−$C_{hex}$][a] (Å) | number of imaginary frequency |
|---|---|---|---|---|---|
| Li on model 1-A | *t* site | +105 | +0.5451 | 2.03 | 2 |
| | *b* site | +115 | +0.5448 | 1.98 | 1 |
| | *m* site | +131 | +0.4320 | 1.71 | 0 |
| Li on model 1-B | *m* site | +62.0 | +0.4357 | 1.74 | 0 |

[a] The distance between M and the graphite plane.

favorable position for Li atom adsorption with both models 1-A and 1-B, while the *t* site is the favorite site for H atom adsorption, which is consistent with that reported in the literature as mentioned earlier; (2) the adsorption energy of H atom is slightly higher than that of Li atom, or H atom adsorption is relatively more thermodynamically favorable than Li adsorption; and (3) during the adsorption of Li and H atoms, there is more charge transferred from the former to graphite, although the latter's adsorption is stronger. This means that the stability of adsorption cannot be judged only by the transferred charges. Another example is that H atom adsorption on the *b* site of model 1-B results in more charge transfer than on the *t* site of the same model structure, as shown in Table 1, but the latter adsorption is more stable.

To clarify the reason the H atom prefers to adsorb on the *t* site of model 1-A or 1-B while the Li atom prefers the *m* site, the electronic structures of models 1-A and 1-B are calculated. Figure 2 shows the contour values of the electrostatic potentials of models 1-A and 1-B. In both models, the *m* site has the highest electrostatic potential, while the *t* site has the lowest electrostatic potential. The reason is apparently due to the highest electron density around *t* site but the lowest electron density around *m* site. Li has a much lower electronegativity (1.0 based upon Pauling scale) and has a strong tendency to contribute electron density in adsorption, thus showing preference for the highest electrostatic potential adsorption site (or the *m* site). In contrast, H has an electronegativity (2.1 according to Pauling scale) comparable to that of C (2.5 according to Pauling scale), preferring to form a covalent bond with the C atom in adsorption. Therefore, H prefers the *t* site near the carbon atom, which has higher electron density or lower electrostatic potential than the *b* or *m* site. This is the reason Li prefers the *m* site but the *t* site is the favorite for H atom adsorption on the basal plane of graphite. The lower electronegativity of Li can also explain the greater transferred charge from Li to graphite than from H to graphite. The covalent C−H bond formed during H atom adsorption is the reason H atom adsorption is stronger than Li atom adsorption. Thus, the different adsorption characters of H and Li atoms on graphite are essentially attributed to their different electronic structures.

From Table 1, one can see that the adsorption energies of a single H atom on models 1-A and 1-B are very different. A similar difference is observed for the single Li atom adsorption on models 1-A and 1-B as shown in Table 2. As mentioned above, the reason is that the single H or Li atom adsorption changes the spin state of the original graphite model. We thus calculated the adsorption of two or four H atoms, which do not change the spin state of the original graphite model. The results are shown in Figure 3. The H atoms still prefer the *t* sites. The adsorption energies of H atoms on models 1-A and 1-B (calculated as per H atom) are all close despite that models 1-A and 1-B have different sizes and different spin states. Our calculated adsorption energy is also in good agreement with that by Bauschlicher,[22] who used a two-level ONIOM method (the Universal Force Field for the low-level treatment and B3LYP/4-31g for the high level description) to study the adsorption of different numbers of H atoms on the sidewall of a large (10,0) single carbon nanotube. The adsorption energy of two H atoms on the carbon nanotube by Bauschlicher was 166 kJ/mol H. The consistent hydrogen adsorption energies from models 1-A and 1-B and the agreement between our results and Bauschlicher's results strongly support the validity of our selected theory and molecular structures for the modeling of hydrogen adsorption on the basal plane of graphite. Despite the extensive theoretical studies in the past several decades, no direct experimental results have been reported about the adsorption energy of the hydrogen atom (or molecules) on the basal plane of graphite. Orimo et al.[23] tested the hydrogen desorption profile of nanostructured graphite prepared by the mechanical milling of graphite under a hydrogen pressure of 1 MPa. Two hydrogen desorption peaks were observed: one at 800 K corresponding to a desorption activation energy of 124 kJ/mol and another one at 1200 K relating to a desorption energy of 244 kJ/mol. On the basis of our calculations, we suggest that the first peak at 800 K may be related to the hydrogen desorption from the basal plane sites and the second peak may be related to the

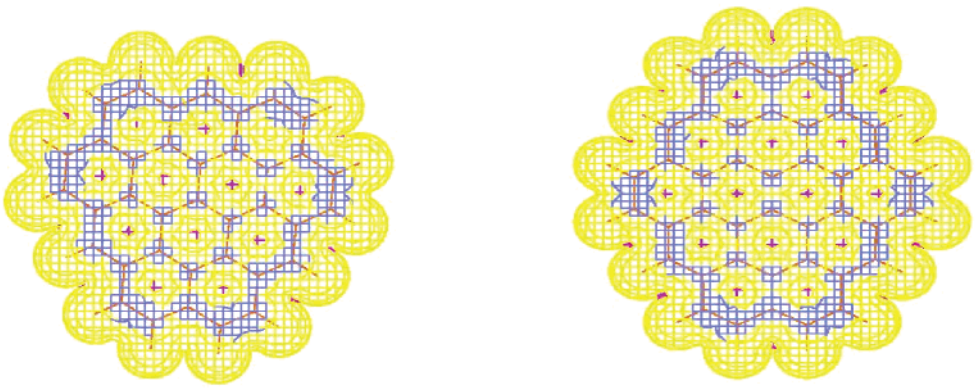


**Figure 2.** Contour values of electrostatic potential of models 1-A and 1-B (pink, 0.5−1.0; yellow, 0.0−0.5; blue, −0.5 to 0.0).

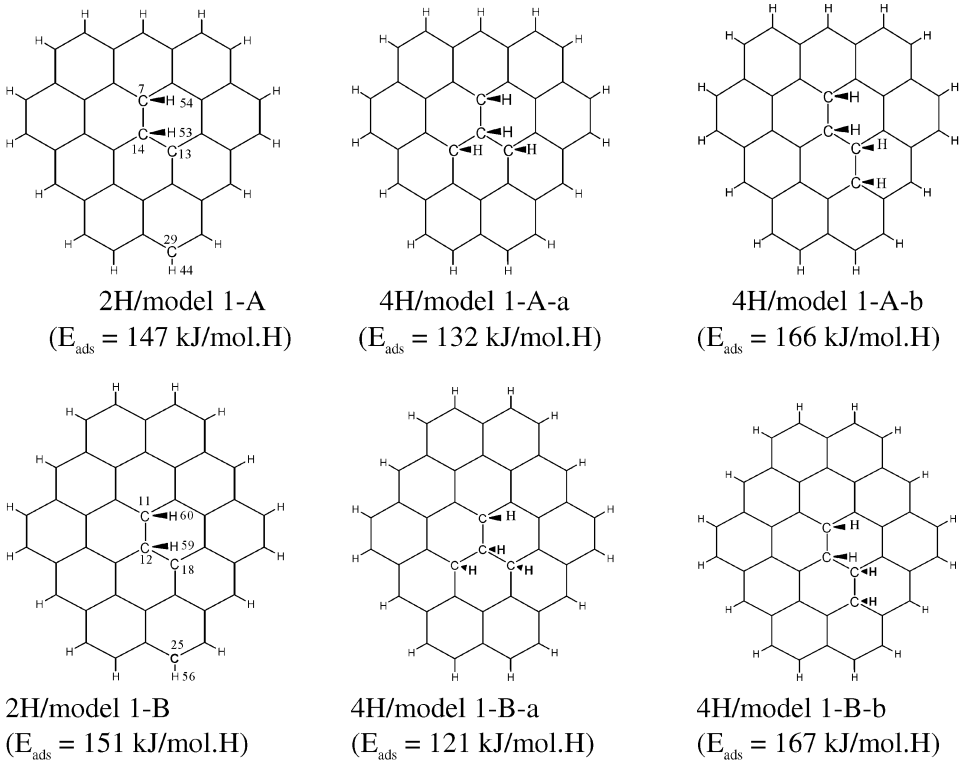


**Figure 3.** Adsorption of two or four H atoms on models 1-A and 1-B.

**TABLE 3: NBO Results for Two H Atoms Adsorption on Models 1-A and 1-B in Figure 3**

| | bond name | bond occupancy[a] | electron density contribution to the bond by each bond atom (%) |
|---|---|---|---|
| two H atoms on *t* site of model 1-A | C(7)−H(54) | 0.9779 | C(7): 62.77<br>H(54): 37.23 |
| | C(7)−C(14) | 0.9874 | C(7): 49.73<br>C(14): 50.07 |
| | C(14)−H(53) | 0.9690 | C(14): 63.90<br>H(53): 36.10 |
| | C(14)−C(13) | 0.9841 | C(14): 50.51<br>C(13): 49.49 |
| | C(29)−H(44) | 0.9907 | C(29): 61.83<br>H(44): 38.17 |
| two H atoms on *t* site of model 1-B | C(12)−H(59) | 1.9400 | C(12): 63.77<br>H(59): 36.23 |
| | C(12)−C(18) | 1.9688 | C(12): 50.54<br>C(18): 49.55 |
| | C(12)−C(11) | 1.9737 | C(12): 50.00<br>C(11): 50.00 |
| | C(25)−H(56) | 1.9810 | C(25): 61.86<br>H(56): 38.14 |

[a] 2H/model 1-A has an open-shell elelectronic state; its bond occupancy is characterized by α electrons, which is one-half that of 2H/model 1-B, while the latter has a closed-shell electronic state.

hydrogen desorption from edge sites. Considering that the desorption experiment by Orimo et al. was conducted in a flowing gas phase, the desorption energy of hydrogen atoms from the basal plane of graphite should be relatively higher than 124 kJ/mol in a static environment. Our calculated adsorption energy of hydrogen atom(s) is ca. 120−160 kJ/mol H. As hydrogen desorption is actually an inverse process of hydrogen adsorption, the experimental results by Orimo et al. provide a good experimental support to our theoretical calculations (although indirectly).

Our recent study[15] has showed that the density functional theory method is better than the MP2 method in modeling a single alkali metal atom adsorption on the basal plane of graphite, and consistent adsorption energy can be achieved if the size of the graphite structure (with the same spin state) is no less than 10 aromatic rings (to form the big $\pi$ band on the basal plane). We also calculated the adsorption of two or four Li atoms, which still prefer the *m* sites (not strictly at the middle point of the aromatic ring), but a slight change of the initial positions of the Li atoms in the input file leads to very different adsorption energies. This means that the current theoretical method is not good enough to model the adsorption of two or four Li atoms (or more than one Li) on the basal plane of graphite. One important reason is that density functional theory is not suitable for modeling the weak (but not negligible) interaction between the Li atoms. The MNDO method was used by Kurita et al.[14] to model the adsorption of more than one Li atom on the basal plane of a single layer graphite (the largest

graphite structure size by them was $C_{54}H_{18}$), and the adsorption energies varied from 120 to 340 kJ/mol Li when the number of Li atoms increased from 2 to 6, and the Li atoms always moved to the areas next to the edge sides, which are not on the "real" basal plane due to the electronic affection by the edge sites. So far, it is agreed that alkali metal atoms prefer the *m* sites of the graphite basal plane, but how to theoretically model more than one alkali metal atom adsorption on the graphite basal plane still remains a challenge.

The covalent character of the formed C−H bond on the basal plane of graphite is another interesting issue. To confirm such as character, NBO (Natural Bond Orbitals) calculations were conducted, and the results of two H atoms adsorption are shown in Table 3. For two H atoms adsorption on the *t* sites of model 1-A, the occupancy of the bond C(7)−H(54) on the basal plane is 0.9779, of which 62.77% electron density contribution is from C(7), and 37.23% is from H(54). The occupancy of the covalent bond C(29)−H(44) on the edge site is just slightly higher (0.9907), 61.83% from C(29) and 38.17% from H(44). Apparently, the character of the bond C(7)−H(54) on the basal plane is similar to that of the covalent bond C(29)−H(44) on the edge site, except that the latter is relatively stronger. This confirms the covalent bond character formed by the H atom adsorption on the *t* site of the graphite basal plane. Similar observations can be made on two H atoms adsorption on model 1-B. It is noteworthy that as the structure 2H/model 1-A (i.e., two H atoms adsorbed on model 1-A) has an open-shell electronic state, the corresponding occupancy listed in Table 3 is characterized only by $\alpha$ electrons, which is one-half of the bond occupancy of 2H/model 1-B. The latter has a closed-shell electronic state. Yet this does not affect the analysis of the bond character. We also conducted NBO calculations on a single H atom adsorption on models 1-A and 1-B, and similar results were obtained. Yet when we calculated NBO for a single Li atom adsorption on the basal plane of models 1-A and 1-B, we found that no chemical bond is formed between Li and any C atom in the graphite sheet. This is consistent with Li atom adsorption on the basal plane of graphite being much weaker than hydrogen atom adsorption.

**Acknowledgment.** Financial support for this project was provided by the Australian Research Council Discovery Grant (APD for Z.H.Z.). This work is also partially supported by the Australian Research Council Centre for Functional Nanomaterials under its Centre of Excellence Scheme.

## References and Notes

(1) Bennett, A. J.; McCarroll, B.; Messmer, R. P. *Surf. Sci*. **1971**, *24*, 191.
(2) Dovesi, R.; Pisani, C.; Ricca, F.; Roetti, C. *J. Chem. Phys.* **1976**, *65*, 3075.
(3) Caballol, R.; Igual, J.; Illas, F.; Rubio, J. *Surf. Sci.* **1985**, *149*, 621.
(4) Barone, V.; Lelj, F.; Minichino, C. *Surf. Sci.* **1987**, *189*, 185.
(5) Jeloaica, L.; Sidis, V. *Chem. Phys. Lett.* **1999**, *300*, 157.
(6) Yang, F. H.; Yang, R. T. *Carbon* **2002**, *40*, 437.
(7) Ferro, Y.; Marinelli, F.; Allouche, A. *J. Chem. Phys*. **2002**, *116*, 8124.
(8) Zhu, Z. H.; Yang, R. T.; Lu, G. Q. *Carbon* **2003**, *41*, 635.
(9) Chen, P.; Wu, X.; Lin, J.; Tan, K. L. *Science* **1999**, *285*, 91.
(10) Zhu, Z. H.; Lu, G. Q.; Smith, S. C. *Carbon* **2004**, *42*, 2509.
(11) Yang, R. T. *Carbon* **2000**, *38*, 623.
(12) Janiak, C.; Hoffman, R.; Sjövall, P.; Kasemo, B. *Langmuir* **1993**, *9*, 3427.
(13) Lamoen, N.; Persson, B. N. J. *J. Chem. Phys.* **1998**, *108*, 3332.
(14) (a) Kurita, N. *Carbon* **2000**, *38*, 65. (b) Kurita, N.; Endo, M. *Carbon* **2002**, *40*, 253.
(15) Zhu, Z. H.; Lu, G. Q. *Langmuir* **2004**, *20*, 10751.
(16) Frisch, M. J.; Trucks, G. W.; Schlegel, H. B.; Scuseria, G. E.; Robb, M. A.; Cheeseman, J. R.; Zakrzewski, V. G.; Montgomery, J. A., Jr.; Stratmann, R. E.; Burant, J. C.; Dapprich, S.; Millam, J. M.; Daniels, D.; Kudin, K. N.; Strain, M. C.; Farkas, O.; Tomasi, J.; Barone, V.; Cossi, M.; Cammi, R.; Mennucci, B.; Pomelli, C.; Adamo, C.; Clifford, S.; Ochterski, J.; Petersson, G. A.; Ayala, P. Y.; Cui, Q.; Morokuma, K.; Malic, D. K.; Rabuc, A. D.; Raghavachari, K.; Foresman, J. B.; Cioslowski, J.; Ortiz, J. V.; Baboul, A. G.; Stefano, B.; Liu, G.; Liashenko, A.; Piskorz, P.; Komaromi, I.; Gomperts, R.; Martin, R. L.; Fox, D. J.; Keith, T.; Al-Laham, M. A.; Peng, Y.; Nanayakkara, A.; Gonzalez, C.; Challacomb, M.; Gill, P. M. W.; Johnson, B.; Chen, W.; Wong, M. W.; Andres, J. L.; Gonzalez, M.; Replogle, E. S.; Pople, J. A. *Gaussian 98*, revision A.7; Gaussian, Inc.: Pittsburgh, PA, 1998.
(17) Foresman, J. B.; Frisch, A. *Exploring Chemistry with Electronic Structure Methods*, 2nd ed.; Gaussian: Pittsburgh, PA, 1996.
(18) Montoya, A.; Trong, T. N.; Sarofim, A. F. *J. Phys. Chem. A* **2000**, *104*, 6108.
(19) Zhu, Z. H.; Lu, G. Q.; Yang, R. T.; Wilson, M. A. *Energy Fuels* **2002**, *16*, 847.
(20) Kyotani, T.; Tomita. *J. Phys. Chem. B* **1999**, *103*, 3434.
(21) *Handbook of Chemistry and Physics*, 67th ed.; CRC Press: Cleveland, OH, 1978; p F158.
(22) Bauschlicher, C. W., Jr. *Chem. Phys. Lett*. **2000**, *322*, 237.
(23) Orimo, T.; Matsushima, F. H.; Fukunaga, T.; Majer, G. *J. Appl. Phys.* **2001**, *90*, 1545.